

Physiologic systemic iron metabolism in mice deficient for duodenal Hfe

Maja Vujic Spasic,^{1,2} Judit Kiss,^{1,2} Thomas Herrmann,³ Regina Kessler,² Jens Stolte,⁴ Bruno Galy,⁴ Birgit Rathkolb,⁵ Eckhard Wolf,⁵ Wolfgang Stremmel,³ Matthias W. Hentze,^{1,4} and Martina U. Muckenthaler^{1,2}

¹Molecular Medicine Partnership Unit, University of Heidelberg, Germany; ²Department of Pediatric Oncology, Hematology, and Immunology, University of Heidelberg, Germany; ³Department of Internal Medicine IV, University of Heidelberg, Germany; ⁴European Molecular Biology Laboratory (EMBL), Heidelberg, Germany; ⁵German Mouse Clinic and Institute of Molecular Animal Breeding and Biotechnology, Ludwig-Maximilian-University, Munich, Germany

Mutations in the *Hfe* gene result in hereditary hemochromatosis (HH), a disorder characterized by increased duodenal iron absorption and tissue iron overload. Identification of a direct interaction between Hfe and transferrin receptor 1 in duodenal cells led to the hypothesis that the lack of functional Hfe in the duodenum affects TfR1-mediated serosal uptake of iron and misprogramming of the iron absorptive cells. Contrasting this view, Hfe deficiency causes inappropriately low expression of the hepatic iron hormone hepcidin,

which causes increased duodenal iron absorption. We specifically ablated Hfe expression in mouse enterocytes using Cre/LoxP technology. Mice with efficient deletion of Hfe in crypt- and villi-enterocytes maintain physiologic iron metabolism with wild-type unsaturated iron binding capacity, hepatic iron levels, and hepcidin mRNA expression. Furthermore, the expression of genes encoding the major intestinal iron transporters is unchanged in duodenal Hfe-deficient mice. Our data demonstrate that intestinal Hfe is dispensable for the physiologic control of systemic iron homeostasis under steady state conditions. These findings exclude a primary role for duodenal Hfe in the pathogenesis of HH and support the model according to which Hfe is required for appropriate expression of the “iron hormone” hepcidin which then controls intestinal iron absorption. (Blood. 2007;109:4511-4517)

nal Hfe is dispensable for the physiologic control of systemic iron homeostasis under steady state conditions. These findings exclude a primary role for duodenal Hfe in the pathogenesis of HH and support the model according to which Hfe is required for appropriate expression of the “iron hormone” hepcidin which then controls intestinal iron absorption. (Blood. 2007;109:4511-4517)

© 2007 by The American Society of Hematology

Introduction

Because there is no known physiologic pathway for iron excretion, intestinal iron absorption must be tightly controlled to maintain iron balance in the organism. Dietary iron is primarily absorbed in the duodenum, where it is reduced to its ferrous form (Fe²⁺), most likely by the activity of the intestinal brush border ferric reductase Dcytb (Cybrd1), to be transported across the intestinal membrane by the apical permease DMT1 (DCT1, Nramp2, Slc11a2). Alternatively, enterocytes acquire iron by taking up dietary heme, possibly via the newly identified transporter HCP.¹ Absorbed iron is then transferred across the basolateral membrane by the iron export protein ferroportin (Ireg1, MTP1, and Slc11a3). During export, ferrous iron is oxidized by the ferroxidase hephaestin to bind to transferrin for transport in the blood. In healthy subjects the intestinal iron transport machinery is adjusted in conditions of systemic iron deficiency and iron overload to maintain adequate iron supply.^{2,3} However, patients with hereditary hemochromatosis (HH) show progressive iron overload as a consequence of increased intestinal iron absorption. The majority of these patients are homozygous for a missense mutation (C282Y) in the *HFE* gene, which codes for an atypical MHC class I molecule.⁴ Mice homozygous for a null allele of *Hfe*⁵⁻⁷ or the orthologous disease mutation (*Hfe*^{845A/845A})⁸ develop iron overload that recapitulates human HH.

In the small intestine, Hfe is found in duodenal crypt cells,⁹ as well as within the extreme apical cytoplasm of intestinal villus enterocytes,¹⁰ and its expression appears to be regulated in response to iron overload.¹¹ Moreover, transgenic overexpression

of *Hfe* in mature duodenal enterocytes produced hepatic iron overload in the mouse, suggesting that Hfe can operate within these cells to augment iron absorption.¹² Whether expression of Hfe at physiologic levels affects iron absorption is still unknown. Based on the findings that (1) Hfe protein is expressed in duodenal crypt cells where it can interact with the coexpressed transferrin receptor 1 (TfR1)⁹ and (2) Hfe competes with transferrin for binding to TfR1 to modulate cellular iron uptake,¹³⁻¹⁵ it has been hypothesized that crypt stem cells could use the Hfe-TfR1 complex to sense systemic iron availability (ie, the amount of iron bound to plasma transferrin) and subsequently program the expression of iron transporters in the absorptive progeny cells of the villi.¹⁶

Both in patients and mice, *HFE* deficiency correlates with inappropriately low basal expression of the hepatically expressed iron-hormone hepcidin (LEAP1, Hamp)¹⁷⁻²⁰ that fails to be adjusted appropriately in response to elevated hepatic iron levels in mice.^{18,19} Hepcidin is a β -defensin-like polypeptide whose expression is normally increased in response to secondary iron overload and which inhibits iron release from duodenal enterocytes (and also macrophages and hepatocytes) by inducing the lysosomal degradation of the iron exporter ferroportin.²¹ Thus, an alternative model for *HFE* function suggests that the inappropriately low-hepcidin levels in HH trigger increased iron absorption by elevated expression of ferroportin.

To differentiate between the 2 models for *HFE*-mediated HH, and to study the in vivo function of Hfe in the duodenum, we used the Cre/loxP technology and established a mouse line with

Submitted July 21, 2006; accepted October 30, 2006. Prepublished online as *Blood* First Edition Paper, January 30, 2007; DOI 10.1182/blood-2006-07-036186.

An Inside *Blood* analysis of this article appears at the front of the issue.

The publication costs of this article were defrayed in part by page charge payment. Therefore, and solely to indicate this fact, this article is hereby marked “advertisement” in accordance with 18 USC section 1734.

© 2007 by The American Society of Hematology

selective and complete *Hfe* deficiency in intestinal crypt and villus enterocytes. We show that duodenal *Hfe* is dispensable for physiologic iron homeostasis under steady state conditions, excluding one of the previously favored models for HH.

Materials and methods

Mice

The generation of mice carrying a null (*Hfe*^{-/-}) or a “floxed” (*Hfe*^{lox}) *Hfe* allele was described previously.⁷ In *Hfe*^{lox} mice, exons 3 to 5 are flanked with 2 loxP sites; *Cre*-mediated excision of these exons has been shown to generate an *Hfe* null allele.⁷ Selective *Hfe* ablation in enterocytes of the intestine was achieved by crossing *Hfe*^{lox} mice with a transgenic line (B6SJL-Tg(Vil-Cre)997Gum; Jackson Laboratory, Bar Harbor, ME) expressing the *Cre* recombinase under the control of promoter elements of the murine *Villin* gene to obtain *Hfe*^{VillinCre} mice.²²

Mice were genotyped by polymerase chain reaction (PCR) analysis of genomic DNA extracted from the tail tip using the DNeasy kit (Qiagen, Hilden, Germany). PCR conditions were as follows: 95°C for 5 minutes, (95°C for 1 minute, 63°C for 1 minute, 72°C for 1 minute) for 30 cycles. Primers used to detect the full-length *Hfe*^{lox} allele were F and R1. Primers used to detect the truncated allele were F and R2. Primers used to detect the *Cre* transgene were Cre3 and Cre5. Primer locations are indicated in Figure 1A and primer sequences are given in Table 1. PCR products were resolved on 1.5% agarose gels and visualized by ethidium-bromide staining.

Hfe^{-/-} and *Hfe*^{lox} mice on a mixed genetic background (C57BL/6 × 129P2/OlaHsd⁷) were back-crossed to the C57BL/6 genetic background. *Hfe*^{VillinCre} mice of both sexes were analyzed at 18 to 22 weeks of age. Wild-type age- and sex-matched C57BL/6 mice were used as controls throughout the study. All mice were born and housed in the SPF animal facility of the EMBL. They were maintained on a standard mouse diet containing 225 mg/kg iron (Teklad 2018 S; Harlan Winkelmann, Borchen, Germany) on average and a constant dark-light cycle and allowed continuous access to food. Mice were killed by CO₂ inhalation. Heparinized blood was collected by cardiac puncture. Longitudinal sections of the proximal duodenum were collected first, then other tissues were collected. All mouse breeding and animal experiments were approved by and in compliance with the guidelines of the Institutional Animal Care and Use Committee of the EMBL.

Table 1. List of primers used

Primer name	Sequence
Genomic PCR*	
F1	5'-CACAGTAAGGGTACGTGGAG-3'
R1	5'-TGGAGACAGTGCAGTAGAGC-3'
R2	5'-AGGGTCACAAACAGCCATAC-3'
<i>Cre</i> 3 forward	5'-TTGGCTGCATACCGGTTCATGCA-3'
<i>Cre</i> 5 reverse	5'-TCGGATCCGCCGATAACCAG-3'
Quantitative real-time PCR†	
<i>Hamp</i> forward	5'-GGGGGATATCAGGCCTCTGCACAGCAGAACAAGG-3'
<i>Hamp</i> reverse	5'-GGGGGATATCAGGCCTCTATGTTTTGCAACAGATACC-3'
<i>Dcytb</i> forward	5'-CTCTTCGGAACAGTGATGCGA-3'
<i>Dcytb</i> reverse	5'-GGGTGTTTCAGGACAAAGAACAG-3'
Ferroportin forward	5'-TGTCAGCCTGCTGTTTCAGGA-3'
Ferroportin reverse	5'-TCTTGCAGCAACTGTGTCCAGC-3'
<i>Dmt1</i> forward	5'-GTGGTGGCTGCAGTGGTTACGG-3'
<i>Dmt1</i> reverse	5'-TTGCCACCGCTGGTATCTTCGC-3'
<i>Gapdh</i> forward	5'-GTGGAGATTTGTTGCCATCAACGA-3'
<i>Gapdh</i> reverse	5'-CCCATCTCCGGCTTGACTGT-3'

*Primers used for genotyping and establishment of *Hfe* recombination efficiency.

†Primers used for gene expression analysis by quantitative real-time PCR.

Enterocyte preparation by laser capture microdissection

The duodenum was dissected from each mouse, opened longitudinally, placed on a piece of aluminum foil, and immediately frozen in liquid nitrogen. Samples were stored at -80°C until further use. Microdissection was carried out on 5-μm thin duodenal tissue sections cut on 1 mm polyethylenepthalate membrane on glass slides (P.A.L.M. Laser Microscopy System, Zeiss Axiovert 135 microscope, 337 nm laser, intensity 1012 W/m²; Zeiss, Jena, Germany). DNA was isolated by lysing the captured cells overnight at 37°C in a buffer containing 0.04% Proteinase K, 10 mM Tris-HCl pH 8.0, 1 mM EDTA, 1% Tween-20. PCR analysis was performed under the conditions described for genotyping.

Measurements of tissue nonheme iron content

Nonheme iron content of liver and duodenal tissues was measured by a slight modification of the method described by Torrence and Bothwell.²³ Briefly, tissues were dried (72 hours at 42°C) and digested in 10% TCA/10% HCl (48 hours at 65°C). Tissue debris was pelleted by centrifugation (15 700g for 5 minutes). Twenty microliters of 10 × diluted supernatant was added to 100 μL chromogenic solution (6 M Na acetate/0.01% bathophenanthroline-disulfonic acid/0.1% thioglycolic acid) in a 96-well plate and incubated for 10 minutes at room temperature. Absorbance (535 nm) was measured in a photometer (SpectramaxPlus; Molecular Devices, Munich, Germany). Iron content was calculated using serial dilution of an iron-standard (Iron atomic absorption standard solution; Sigma-Aldrich, Deisenhofen, Germany); values are expressed as micrograms of iron per gram of dry tissue.

Measurements of serum iron parameters

Serum samples have been analyzed by the clinical-chemical laboratory of the German Mouse Clinic²⁴ using the AU400-System (Olympus Diagnostica, Hamburg, Germany) and adapted reagents (Olympus Diagnostica) according to the manufacturer's instructions to determine serum iron (OSR6186) and ferritin (OSR6150) concentrations as well as the UIBC (OSR6124).

RNA extraction, reverse transcription, and real-time PCR

Total RNA was isolated using Trizol reagent, and 2 μg total RNA was reverse transcribed using the Revertaid H Minus M-MuLV Reverse Transcriptase (Fermentas, Hanover, MD) following the manufacturer's instructions. Quantitative real-time PCR was carried out in 25-μL reaction volume using SYBR Green I dye on ABI Prism 7500 (Applied Biosystems, Applied Biosystems, Weiterstadt, Germany). Primers were designed to specifically amplify hepcidin, *Dcytb*, *DMT1*, *Ireg1*, and *Gapdh* sequences. Primer sequences are indicated in Table 1. Amplification conditions were as follows: 50°C for 2 minutes, 95°C for 10 minutes (95°C for 15 seconds, 60°C for 15 seconds) for 45 cycles. The mRNA abundance of each transcript was calculated relative to the expression of the housekeeping gene *Gapdh* (glyceraldehyde-3-phosphate-dehydrogenase). Data have been analyzed using the modified REST program,²⁵ which allows analyzing the expression of a target gene standardized by a nonregulated reference gene. The mathematical model used is based on the correction for exact PCR efficiencies and the mean crossing point deviation between sample group(s) and control group(s).

Results

Generation of mice with selective *Hfe* deficiency in intestinal enterocytes (*Hfe*^{VillinCre})

To assess whether *Hfe* expression in the intestine contributes to the maintenance of murine iron homeostasis, we used the *Cre/loxP* technology²² to establish a mouse line that lacks *Hfe* selectively in the small intestine but not in other tissues. We used a previously generated mouse line carrying a floxed *Hfe* allele (*Hfe*^{lox}), in which

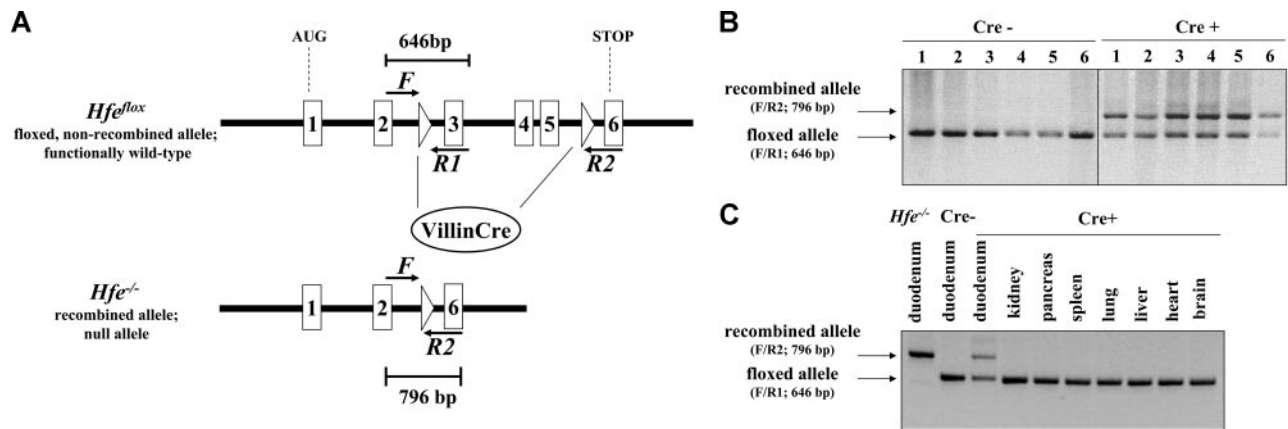


Figure 1. Generation of *Hfe*^{VillinCre} mice. (A) Duodenum-specific *Hfe* knock-out mice were generated by crossing mice carrying a floxed *Hfe* allele (*Hfe*^{flox}) with mice expressing the *Cre* recombinase under the control of the murine villin promoter. *Cre*-mediated excision of exons 3 to 5 generates an *Hfe* null allele. PCR primers F and R1 amplify a 646-bp (base pair) fragment from the intact *Hfe*^{flox} allele, whereas primers F and R2 amplify a 796-bp fragment from the recombined allele. Under the PCR conditions used, these primers fail to amplify the predicted 2827-bp fragment from the full-length *Hfe*^{flox} allele. Exons are symbolized by numbered boxes, triangles indicate the loxP sites. (B) The *Hfe*^{flox} allele is recombined specifically in the intestine. Recombination of the *Hfe*^{flox} allele along the intestinal axis in *Hfe*^{VillinCre} mice expressing the *Cre* recombinase (*Cre*⁺) and in control littermates (*Cre*⁻) is monitored by PCR analysis using the primers detailed in Figure 1A. The numbers above each lane refer to the corresponding intestinal sections: 1, 0 to 2 cm; 2, 2 to 4 cm; 3, 4 to 6 cm; 4, 6 to 8 cm; 5, 8 to 10 cm; 6, 10 to 12 cm downstream of the pylorus. (C) Tissue specificity of *Hfe* recombination was assessed by diagnostic PCR analysis. The duodenum samples correspond to the proximal 2 cm of the intestine. *Hfe*^{-/-} and *Hfe*^{flox} (*Cre*⁻) samples were used as positive and negative controls, respectively.

exons 3 to 5 are flanked with loxP sites⁷ (Figure 1A). Global *Cre*-mediated excision of exons 3 to 5 in this line generates an *Hfe*-null allele and recapitulates the phenotype seen in HH.⁷ The *Hfe*^{flox} mouse line was crossed with transgenic mice expressing the *Cre* recombinase under the control of the murine *Villin 1* promoter²⁶ to generate *Hfe*^{VillinCre} mice (Figure 1A). *Hfe*^{VillinCre} mice are viable, fertile, normal in size, and do not display any overt physical or behavioral abnormality (data not shown).

Tissue specificity of *Hfe* inactivation by the Villin promoter-driven *Cre* transgene was determined by genomic PCR analysis as schematically illustrated in Figure 1A. Recombination of the *Hfe*^{flox} allele is observed along the entire small intestine in *Hfe*^{VillinCre} mice, including the proximal section of the duodenum where most of the iron absorption takes place (Figure 1B). Messenger RNA analysis using primers specific for the wild-type and recombined *Hfe* alleles yielded comparable results (data not shown). As expected, no

recombination of the *Hfe*^{flox} allele is detected in any of the other organs tested (Figure 1C). However, both recombined and non-recombined alleles are detected when analyzing genomic DNA prepared from whole intestinal sections of the *Hfe*^{VillinCre} mice (Figure 1B-C). This indicates either that the recombination of the *Hfe*^{flox} allele in enterocytes is incomplete or that DNA from connective tissue and smooth muscle cells not expressing the *Cre* recombinase contributes to the signal of the intact *Hfe*^{flox} allele (Figure 1B-C). Importantly, only the non-recombined or the fully recombined allele is detected in intestinal samples from *Hfe*^{flox} or *Hfe*^{-/-} mice, respectively (Figure 1C).

Because *Hfe* was suggested to function in crypt and/or villi enterocytes,^{9,10} it is important to determine the efficiency of *Cre*-mediated recombination in both cell types. Therefore, crypt and villus enterocytes were isolated by laser capture microdissection (Figure 2A-D), and recombination efficiency was assessed by

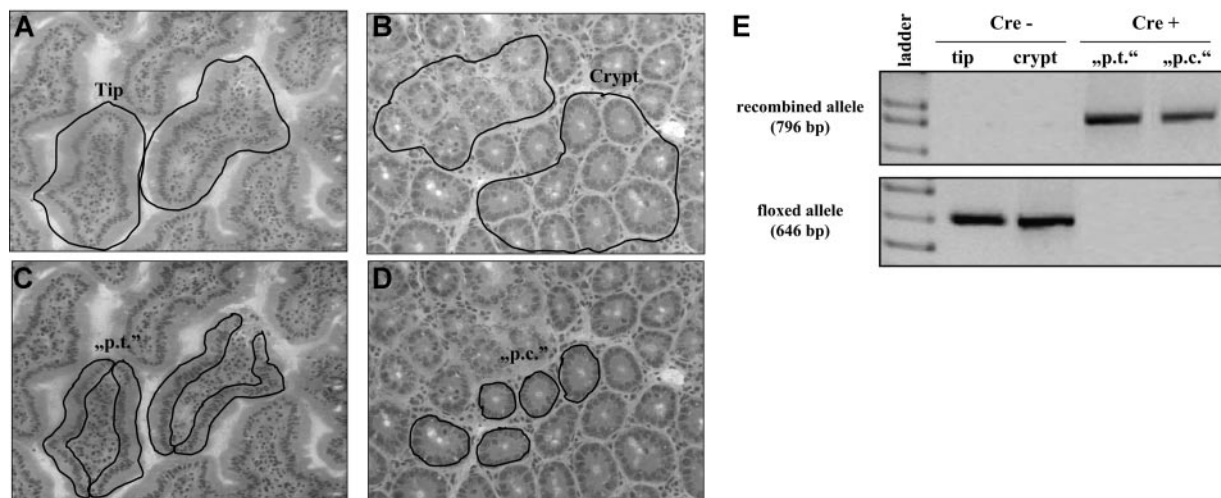


Figure 2. *Cre*-mediated recombination of the *Hfe*^{flox} allele is highly efficient in both duodenal crypt and tip enterocytes. Indicated cell populations were excised by laser capture microdissection of duodenal sections from *Hfe*^{VillinCre} mice (H&E staining; 10×/0.25 NA objective lens on an Olympus BX51 microscope [Olympus, Hamburg, Germany]). (A) Tip enterocytes (tip), (B) crypt enterocytes (crypt), (C) pure tip enterocytes (p.t.) (D), and pure crypt enterocytes (p.c.). (E) PCR analysis of genomic DNA extracted from samples A to D using primers specific for the floxed (F and R1) or the recombined (F and R2) *Hfe* allele. The 1-kb (kilobase) Plus DNA ladder (Invitrogen, Karlsruhe, Germany) was used as a size marker.

Table 2. Nonheme liver iron content, serum iron parameters, and serum ferritin values

Genotype, significance	Liver iron	Serum iron	UIBC	Tf saturation	Ferritin
C57BL/6					
Male	297 ± 36 (6)	254 ± 191 (5)	28 ± 6 (6)	84 ± 10 (6)	60 ± 16 (6)
Female	360 ± 64 (4)	560 ± 68 (4)	26 ± 9 (4)	95 ± 2 (4)	75 ± 15 (4)
<i>P</i> , male vs female	.187	.029	.744	.084	.256
<i>Hfe</i>^{-/-}					
Male	889 ± 233 (9)	347 ± 210 (10)	17 ± 7 (10)	95 ± 2 (10)	69 ± 23 (10)
Female	1376 ± 235 (8)	548 ± 223 (8)	8 ± 3 (5)	92 ± 6 (8)	84 ± 36 (8)
<i>P</i> , male vs female	.001	.086	.005	.249	.376
<i>P</i>, <i>Hfe</i>^{-/-} vs C57BL/6					
Male	< .001	.456	.011	.189	.422
Female	< .001	.901	.032	.816	.610
<i>Hfe</i>^{fllox}, <i>VillinCre</i>⁻					
Male	323 ± 87 (14)	291 ± 175 (12)	29 ± 5 (12)	87 ± 7 (12)	53 ± 18 (12)
Female	434 ± 138 (15)	342 ± 189 (10)	32 ± 8 (10)	88 ± 7 (10)	47 ± 17 (10)
<i>P</i> , male vs female	.013	.538	.371	.783	.492
<i>Hfe</i>^{fllox}, <i>VillinCre</i>⁺					
Male	349 ± 144 (23)	265 ± 185 (14)	29 ± 10 (14)	79 ± 24 (14)	46 ± 9 (14)
Female	519 ± 169 (11)	381 ± 197 (8)	31 ± 4 (8)	89 ± 7 (8)	55 ± 10 (8)
<i>P</i> , male vs female	.013	.228	.435	.268	.098
<i>P</i>, <i>VillinCre</i>⁻ vs <i>VillinCre</i>⁺					
Male	.505	.735	.806	.513	.285
Female	.212	.700	.708	.759	.302

Liver iron content (in μg iron/g dry tissue), serum iron (in $\mu\text{g}/\text{dL}$), unsaturated iron binding capacity (UIBC; in $\mu\text{g}/\text{dL}$), transferrin (Tf) saturation (in %) and serum ferritin (in $\mu\text{g}/\text{L}$) were determined in C57BL/6 wild-type, *Hfe*^{-/-}, and *Hfe*^{VillinCre} mice. Groups of male and female mice are tabulated separately. Results are shown as mean \pm SD to the mean. The sample size is indicated in parentheses; *P* values were calculated using the Student *t* test.

genomic PCR analysis in these samples. For ease of handling, larger tissue regions containing mainly tip (Figure 2A) and crypt enterocytes (Figure 2B) were isolated from mice lacking the *Cre* recombinase transgene (*Cre*⁻), whereas pure tip (p.t.; Figure 2C) and pure crypt (p.c.; Figure 2D) enterocytes were isolated from mice carrying the *Cre* transgene (*Cre*⁺). DNA analysis of these preparations shows that the full-length *Hfe*^{fllox} allele present in *Cre*⁻ mice is absent in both crypt and tip enterocytes of *Cre*⁺ mice where, importantly, only the recombined allele is detected (Figure 2E). This demonstrates that recombination of the *Hfe*^{fllox} allele in mice carrying the *Cre* transgene is highly efficient and specific in crypt and villus enterocytes of the intestine.

Effect of intestinal *Hfe* deficiency on serum iron parameters, hepatic iron levels, and hepcidin mRNA expression

To test whether *Hfe* expression in intestinal enterocytes is required to maintain normal systemic iron homeostasis, we analyzed the liver iron content of *Hfe*^{VillinCre} mice (18-22 weeks of age) expressing the *Cre* transgene (*Cre*⁺) in comparison to *Cre*⁻ littermates. As a positive control for liver iron loading, we used mice derived from the same original line with constitutive *Hfe* deficiency (*Hfe*^{-/-}) (together with age- and sex-matched wild-type mice) whose generation and analysis has been described previously.⁷ As expected, both *Hfe*^{-/-} males and females accumulate significantly more iron in the liver than C57BL/6 control mice (Table 2). *Hfe*^{-/-} females also accumulate significantly more iron in the liver compared with *Hfe*^{-/-} males (1.8-fold; *P* = .001). By contrast, mice with complete and selective *Hfe* deficiency in enterocytes display no hepatic iron accumulation, associated with unchanged serum iron levels, unsaturated iron-binding capacity (UIBC), transferrin saturation, and serum ferritin values. As expected, the UIBC is reduced in *Hfe*^{-/-} male and female mice compared with respective wild-type controls (Table 2).

Previous work showed increased hepcidin mRNA expression in response to secondary iron overload, but a failure to increase hepcidin in response to the primary iron overload caused by *Hfe* deficiency.^{7,10} Consistently, *Hfe*^{-/-} mice lack a significant increase in hepcidin mRNA expression (Figure 3) despite increased hepatic iron levels (Table 2). Importantly, and in agreement with the other systemic iron homeostasis parameters, *Hfe*^{VillinCre} *Cre*⁺ and *Cre*⁻ mice show comparable hepcidin mRNA expression (Figure 3). However, hepcidin mRNA levels are 2-fold higher in female mice compared with males independent of the genotype (Figure 3), correlating with elevated liver iron content in female mice (Table 2).

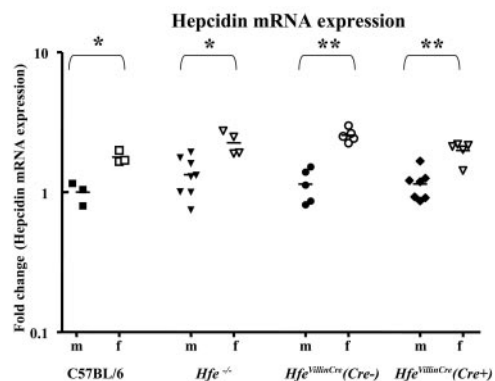


Figure 3. Hepatic hepcidin mRNA expression. Hepcidin mRNA expression was measured in age- and sex-matched C57BL/6, *Hfe*^{-/-}, and *Hfe*^{VillinCre} mice by quantitative real-time PCR using primers that specifically amplify both murine hepcidin isoforms. Groups of male (m) and female (f) mice are represented separately. Mean hepcidin mRNA expression in C57BL/6 males was arbitrarily set as 1; all other data are expressed in relation to this. There is no statistically significant difference in hepcidin expression between the different mouse genotypes. However, hepcidin mRNA expression differs significantly between male (m) and female (f) mice within each genotype (**P* < .05; ***P* < .005, Student *t* test). Mean values are represented by horizontal bars.

Taken together, these data show that duodenal *Hfe* expression is dispensable for normal iron homeostasis and liver iron loading under steady state conditions.

Unaltered mRNA expression of duodenal iron transporters in *Hfe^{VillinCre}* mice

To examine whether enterocytic *Hfe* deficiency exerts local effects by modulating the expression of duodenal iron transporters, we assayed the mRNA expression of the brush border ferric reductase Dcytb (Cybrd1), the transmembrane permease DMT1 and the iron export protein ferroportin in the duodenum of C57BL/6, *Hfe^{-/-}*, and *Hfe^{VillinCre}* mice (Cre⁺ and Cre⁻) by quantitative real-time RT-PCR (Figure 4).

As noted before,⁷ we find a significant increase in Dcytb mRNA expression in *Hfe^{-/-}* compared with C57BL/6 wild-type mice, with a more pronounced augmentation in males (3.74-fold; $P = .001$) than in females (1.4-fold; $P = .03$). In contrast, Dcytb mRNA expression remains unchanged both in male and female *Hfe^{VillinCre}* (Cre⁺) mice compared with Cre⁻ littermates. These data strongly suggest that elevated Dcytb mRNA expression in *Hfe^{-/-}* mice is not a primary effect of intestinal *Hfe* deficiency, but rather a consequence of the systemic changes in iron homeostasis associated with constitutive HFE deficiency. DMT-1 and ferroportin mRNA expression also remains unaltered in sex- and age-matched C57BL/6, *Hfe^{-/-}*, and *Hfe^{VillinCre}* mice (Figure 4B-C). Together with an unchanged duodenal iron content (data not shown), our data suggest that duodenal *Hfe* plays no direct role in the local regulation of iron transporter genes in the duodenum.

Discussion

Two opposing models have been discussed for the role of HFE in HH. According to the first, HFE function in duodenal enterocytes is

required for normal intestinal iron absorption, possibly involving the interaction of HFE with TfR1.¹³⁻¹⁵ According to the second, HFE function in a nonintestinal cell (possibly hepatocytes or hepatic macrophages) enables appropriate hepatic hepcidin expression, which in turn determines physiologic iron absorption.

To address these models, we directly investigated the in vivo function of intestinal *Hfe*. We generated *Hfe^{VillinCre}* mice that lack *Hfe* exclusively in the intestine. Using laser capture microdissection and genomic PCR analysis we demonstrate that the floxed *Hfe* allele is efficiently recombined (close to 100%) in isolated crypt and villi enterocytes (Figure 2). We consider this to be particularly important because (1) in crypt enterocytes, where TfR1 is predominantly expressed,⁹ the Hfe-TfR1 complex has been proposed to serve as part of a sensor mechanism of systemic iron status¹⁶; and (2) transgenic expression of *Hfe* in villi enterocytes has been reported to mediate hepatic iron deposition.¹² Our data show that *Hfe^{VillinCre}* mice (Cre⁺) do not accumulate iron in the liver (Table 2); in addition, they display unaltered UIBC, serum iron, transferrin saturation, and plasma ferritin levels (Table 2) as well as unchanged hepatic hepcidin mRNA expression (Figure 3). These data demonstrate that duodenal *Hfe* is dispensable for normal systemic iron homeostasis in steady state condition. These findings hence refute the hypothesis according to which intestinal *Hfe* function is disturbed in HH.

The transferrin saturation is surprisingly high in C57BL/6 wild-type mice, a finding consistent with data obtained in a previous study.²⁷ The high degree of transferrin saturation in C57BL/6 mice may be related to the iron content of the diet and/or the genetic background of the mice. In addition, and as shown before,²⁸ female mice, compared with their male counterparts, display a higher degree of transferrin saturation (Table 2), correlating with increased serum and hepatic iron levels. The high degree of transferrin saturation observed in C57BL/6 mice may explain the only marginal increase in transferrin saturation

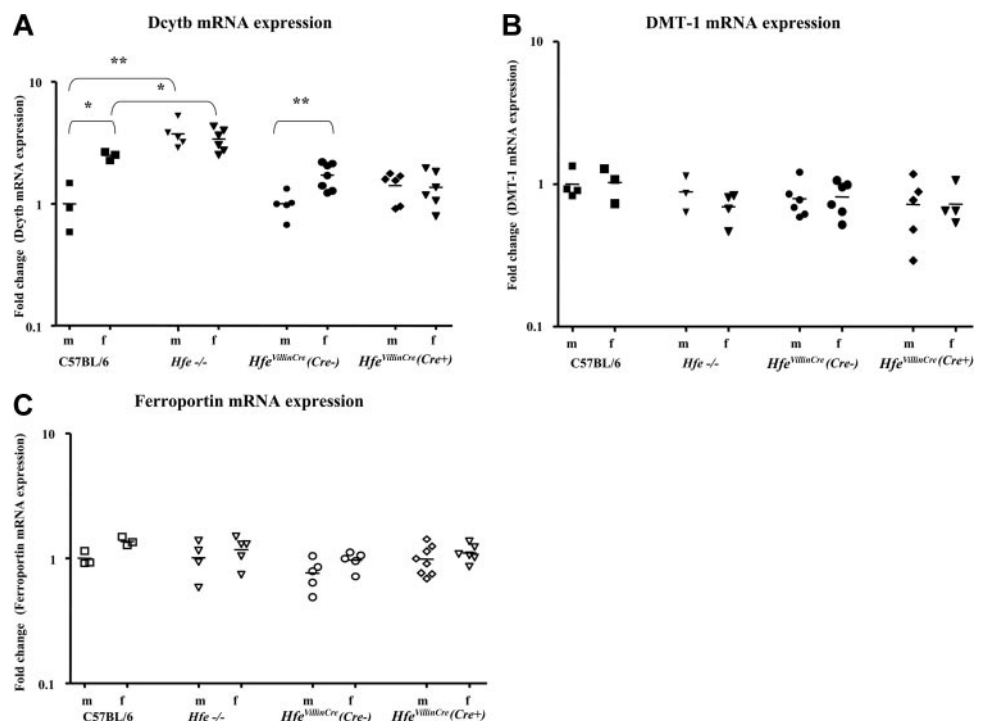


Figure 4. mRNA expression of the intestinal iron transporters. mRNA levels of (A) Dcytb, (B) DMT-1, and (C) ferroportin were measured in age- and sex-matched C57BL/6, *Hfe^{-/-}*, and *Hfe^{VillinCre}* mice by quantitative real-time PCR. Groups of male (m) and female (f) mice are represented separately. Mean mRNA expression in C57BL/6 males was arbitrarily set as 1; all other data are expressed in relation to this. Significant differences in mRNA expression are marked by asterisks (* $P < .05$; ** $P < .005$, Student *t* test). Mean values are represented by horizontal bars.

in male and the lack of increase in female mice with constitutive *Hfe* deficiency.

To assess whether intestinally expressed *Hfe* contributes to the maintenance of local, enterocyte-specific iron homeostasis, we investigated the expression of duodenal iron transporters. Of relevance, increased mRNA expression of DMT-1, ferroportin, and/or *Dcytb* has been reported in the duodenal mucosa of patients with HH and some mouse lines with constitutive *Hfe* deficiency.^{18,29-31} Here, we demonstrate that DMT-1 and ferroportin mRNA expression is unaltered both in constitutive *Hfe*^{-/-} mice as well as in *Hfe*^{VillinCre} (*Cre*⁺) mice compared with their respective controls that were all maintained on a C57BL/6 genetic background. These findings are in line with our previous data showing that DMT-1 mRNA as well as ferroportin mRNA and protein levels remained unchanged in constitutive *Hfe*^{-/-} mice on a mixed C57BL/6 × 129P2/OlaHsd genetic background. In contrast, *Dcytb* mRNA expression was significantly increased in *Hfe*^{-/-} males on a mixed C57BL/6 × 129P2/OlaHsd,^{7,31} in *Hfe*^{-/-} females on the 129S6/SvEvTac¹⁸ and in *Hfe*^{-/-} mice (both male and female) on the C57BL/6 (Figure 4A) genetic backgrounds. *Hfe*^{VillinCre} (*Cre*⁺) mice do not exhibit a significant increase in *Dcytb* mRNA expression compared with their *Cre*⁻ littermates. This finding indicates that regulatory cues induced by the lack of *Hfe* in tissues other than the duodenum (possibly the liver) are responsible for the increased *Dcytb* mRNA expression in *Hfe*^{-/-} mice. We speculate that the low hepatic hepcidin expression resulting from general *Hfe* deficiency increases basolateral iron export from enterocytes via ferroportin. As a consequence the intracellular iron level in enterocytes may be lowered and the increase in *Dcytb* mRNA may reflect a compensatory response. Although increased *Dcytb* expression seems to be a consequence of *Hfe* deficiency, targeted disruption of the *Dcytb* gene in the mouse does not affect systemic and local iron homeostasis parameters.³² To test whether indeed elevated *Dcytb* activity confers the increased iron uptake observed in HH, cross-breeding of *Hfe*^{-/-} and *Dcytb*-deficient mice would be informative.

References

- Shayeghi M, Latunde-Dada G, Oakhill J, et al. Identification of an intestinal heme transporter. *Cell*. 2005;122:789-801.
- Fleming RE, Sly WS. Mechanism of iron accumulation in hereditary hemochromatosis. *Ann Rev Physiol*. 2000;64:663-80.
- Hentze MW, Muckenthaler MU, Andrews NA. Balancing acts: molecular control of iron metabolism. *Cell*. 2004;117:285-297.
- Feder JN, Gnirke A, Thomas W, et al. A novel MHC class I-like gene is mutated in patients with hereditary haemochromatosis. *Nat Genet*. 1996;13:399-408.
- Zhou XY, Tomatsu S, Fleming G, et al. HFE gene knockout produces mouse model of hereditary hemochromatosis. *Proc Natl Acad Sci U S A*. 1998;95:2492-97.
- Bahram S, Gilfillan S, Kühn LC, et al. Experimental hemochromatosis due to MHC class I HFE deficiency: immune status and iron metabolism. *Proc Natl Acad Sci U S A*. 1999;96:13312-13317.
- Hermann T, Muckenthaler M, Hoveen F, et al. Iron overload in adult *Hfe*-deficient mice independent of changes in the steady-state expression of the duodenal iron transporter DMT-1 and *Ireg/ferroportin*. *J Mol Med*. 2004;82:39-48.
- Levy E, Montross LK, Cohen DE, et al. The C282Y mutation causing hereditary hemochromatosis does not produce a null allele. *Blood*. 1999;94:9-11.
- Waheed A, Parkkila S, Saarnio J, et al. Association of HFE protein with transferrin receptor in crypt enterocytes of human duodenum. *Proc Natl Acad Sci U S A*. 1999;96:1579-1584.
- West AR, Thomas C, Sadlier J, Oates PS. Haemochromatosis protein is expressed on the terminal web of enterocytes in proximal small intestine of the rat. *Histochem Cell Biol*. 2005;125:283-292.
- Theurl I, Ludwiczek S, Eller P, et al. Pathways for the regulation of body iron homeostasis in response to experimental iron overload. *J Hepatol*. 2005;43:711-719.
- Fergelot P, Ropert-Bouchet M, Abgueuen E, et al. Iron overload in mice expressing HFE exclusively in the intestinal villi provides evidence that HFE regulates a functional cross-talk between crypt and villi enterocytes. *Blood Cells Mol Dis*. 2002;28:348-360.
- Roy CN, Penny DM, Feder JN, et al. The hereditary hemochromatosis protein, HFE, specifically regulates transferrin-mediated iron uptake in HeLa cells. *J Biol Chem*. 1999;274:9022-9028.
- Salter-Cid L, Brunmark A, Li Y, et al. Transferrin receptor is negatively modulated by hemochromatosis protein HFE: implications for the cellular iron homeostasis. *Proc Natl Acad Sci U S A*. 1999;96:5434-5439.
- Riedel HD, Muckenthaler MU, Gehrke SG, et al. HFE downregulates iron uptake from transferrin and induces iron-regulatory protein activity in stably transfected cells. *Blood*. 1999;94:3915-3921.
- Fleming RE, Migas MC, Zhou X, et al. Mechanism of increased iron absorption in murine model of hereditary hemochromatosis: increased duodenal expression of the iron transporter DMT1. *Proc Natl Acad Sci U S A*. 1999;96:3143-3148.
- Bridle K, Frazer D, Wilkins S, et al. Disrupted hepcidin regulation in HFE-associated haemochromatosis and the liver as a regulator of body iron homeostasis. *Lancet*. 2003;361:669-673.
- Muckenthaler MU, Roy CN, Custodio AO, et al. Regulatory defects in liver and intestine implicate hepcidin and *Cybrd1* gene expression in mouse hemochromatosis. *Nat Genet*. 2003;34:102-107.
- Ahmad KA, Ahmann JR, Migas MC, et al. Decreased liver hepcidin expression in the *Hfe* knockout mouse. *Blood Cells Mol Dis*. 2002;29:361-366.
- Nicolas G, Andrews NC, Kahn A, et al. Hepcidin, a candidate modifier of the hemochromatosis phenotype in mice. *Blood*. 2003;103:2841-2843.
- Nemeth E, Tuttle M, Powelson J, et al. Hepcidin regulates cellular iron efflux by binding to ferroportin and inducing its internalization. *Science*. 2004;306:2090-2093.
- Schwenk F, Baron U, Rajewsky K. A cre-transgenic mouse strain for the ubiquitous deletion of loxP-flanked gene segments including deletion in

Acknowledgments

We thank Vladimir Benes and members of the EMBL Genomics Core Facility for support with qRT-PCR, Dr Gröne and M. Bonrouhi (Deutsches Krebsforschungszentrum [DKFZ]) for help with laser dissection microscopy, and M. Hrabe de Angelis and the German Mouse Clinic for their work. We thank the EMBL transgenic mouse service and the staff of the EMBL animal house for their contribution to this work.

This work was supported by a research grant from the Deutsche Forschungsgemeinschaft (M.U.M.), by a PhD fellowship from the Boehringer Ingelheim Fonds (J.K.), and by the Bundesministerium für Bildung und Forschung (BMBF)/Nationales Genomforschungsnetz (NGFN) (01GR0430) (B.R.).

Authorship

Contribution: M.V.S., J.K., and T.H. participated in designing and performing the research; M.V.S. controlled and analyzed the data; R.K. and J.S. collected data; B.G., B.R., and E.W. centralized the mouse work; W.S., M.W.H., and M.U.M. initiated and conceptualized the work; M.V.S., M.W.H., and M.U.M. wrote the paper; and all authors checked the final version of the manuscript.

Conflict-of-interest disclosure: The authors declare no competing financial interests.

M.V.S., J.K., and T.H. contributed equally to this study. W.S., M.W.H., and M.U.M. also contributed equally to this study.

Correspondence: Martina U. Muckenthaler, University of Heidelberg, Department of Pediatric Oncology, Hematology, and Immunology, Im Neuenheimer Feld 153, 69120 Heidelberg, Germany; e-mail: martina.muckenthaler@med.uni-heidelberg.de; and Matthias W. Hentze, European Molecular Biology Laboratory (EMBL), Meyerhofstrasse 1, 69117 Heidelberg, Germany; e-mail: hentze@embl.de.

- germ cells. *Nucleic Acids Res.* 1995;23:5080-5081.
23. Torrence JD, Bothwell TH. Tissue iron stores. In: Cook JD, Ed. *Methods in Hematology*. New York, NY: Churchill Livingstone Press; 1980:104-109.
24. Gailus-Durner V, Fuchs H, Becker L, et al. Introducing the German Mouse Clinic: open access platform for standardized phenotyping [letter]. *Nat Methods.* 2005;2:403-404.
25. Pfaffl MW, Tichopad A, Prgomet C, et al. Determination of stable housekeeping genes, differentially regulated target genes and sample integrity: BestKeeper-Excel-based tool using pair-wise correlations. *Biotechnol Lett.* 2004;26:509-515.
26. Madison BB, Dunbar L, Qiao XT, et al. *cis* Elements of the villin gene control expression in restricted domains of the vertical (crypt) and horizontal (duodenum, cecum) axes of the intestine. *Biol Chem.* 2002;277:33275-33283.
27. Fleming RE, Holden CC, Tomatsu S, et al. Mouse strain differences determine severity of iron accumulation in Hfe knockout model of hereditary hemochromatosis. *Proc Natl Acad Sci U S A.* 2001;98:2707-2711.
28. Courselaud B, Troadec MB, Fruchon S, et al. Strain and gender modulate hepatic hepcidin 1 and 2 mRNA expression in mice. *Blood Cells Mol Dis.* 2004;32:283-289.
29. Zoller H, Koch RO, Theurl I, et al. Expression of the duodenal iron transporters divalent-metal transporter 1 and ferroportin 1 in iron deficiency and iron overload. *Gastroenterology.* 2001;120:1412-1419.
30. Fleming RE, Migas MC, Zhou X, et al. Mechanism of increased iron absorption in murine model of hereditary hemochromatosis: increased duodenal expression of the iron transporter DMT-1. *Proc Natl Acad Sci U S A.* 1999;96:3143-3148.
31. Zoller H, Pietrangelo A, Vogel W, et al. Duodenal metal-transporter (DMT-1, NRAMP-2) expression in patients with hereditary haemochromatosis. *Lancet.* 1999;353:2120-2123.
32. Gunshin H, Starr CN, DiRenzo C, et al. Cybrd1 (duodenal cytochrome b) is not necessary for dietary iron absorption in mice. *Blood.* 2005;106:4413-4414.